Salt-Bridge Transition State for the Charge Separation $Co(H_2O)_4^{2+} \rightarrow CoOH(H_2O)_2^{+} + H_3O^{+}$

Martin K. Beyer*

Institut für Physikalische und Theoretische Chemie, Technische Universität München, Lichtenbergstrasse 4, 85747 Garching, Germany

Ricardo B. Metz*

Department of Chemistry, University of Massachusetts, Amherst, Massachusetts 01003

Received: September 19, 2002; In Final Form: December 19, 2002

The transition state of the charge separation $Co(H_2O)_4^{2+} \rightarrow CoOH(H_2O)_2^{+} + H_3O^{+}$ is located by density functional theory calculations. The H_3O^{+} unit is already separated from the $CoOH(H_2O)_2^{+}$ moiety by more than 3 Å, and the charge centers form a $Co^{2+}-OH^{-}-H_3O^{+}$ salt bridge, lowering the barrier for the reaction. The transition state is calculated to lie 166 kJ/mol above the products, including zero-point corrections, which compares favorably with the 110 ± 20 kJ/mol kinetic energy release measured in an earlier work (Faherty, K. P.; et al. *J. Phys. Chem. A* **2001**, *105*, 10054). The deviation is interpreted as fractions of the energy going into rotational and vibrational excitation of the products.

Introduction

With the invention of electrospray ionization,[1] solvated doubly charged species became available to ion chemists.[2−5] Because the second ionization potential (IP) of most metals is higher than the first ionization potential of water, the question of the minimum number of solvent molecules required to form a sufficiently stable $M(H_2O)_n^{2+}$ species for mass-spectrometric detection has received considerable attention, beginning with the work of Kebarle and co-workers.[2−4,6,7] The difference in ionization energy between the doubly charged metal and the neutral ligand is responsible for the charge-transfer reaction 1 which was first observed for M = Mg by Spears et al. as early as 1972[8]

$$M^{2+} + H_2O \rightarrow M^{+} + H_2O^{+} \qquad (1)$$

Reaction 1 is the reason for the difficulty of producing $M(H_2O)^{2+}$ by attachment of the ligand to the metal center. When trying to make the target species from larger clusters by collision induced dissociation (CID), charge reduction occurs instead by the thermochemically more favorable proton transfer[2−4]

$$M(H_2O)_n^{2+} \rightarrow MOH(H_2O)_m^{+} + H_3O^{+} + (n - m - 2)H_2O \qquad (2)$$

Reaction 2 has been repeatedly addressed computationally,[9−12] and a more extensive account of these studies is given in a recent review.[13] Calculations for $n = 2$ and M = Be, Mg, Ca, Sr, and Ba have shown that this reaction proceeds via a salt-bridge transition state.[11] The barrier height is directly determined by the ionic radius of the metal. Because the second IP also scales with the ionic radius, the correlation between the occurrence of reaction 2 and the second IP of the metal is only indirect.

In recent photodissociation experiments by Metz and co-workers of $Co(H_2O)_n^{2+}$ ($n = 4-7$)[14] and $Ni(H_2O)_n^{2+}$ ($n = 4-7$),[15] the charge reduction reaction 2 was the dominant reaction observed for $n = 4$, and the kinetic energy release (KER) of the fragment ions was measured. Both the absolute values as well as the narrow distribution of the fragment kinetic energies are in line with the picture of a salt-bridge mechanism. In these experiments, a controlled amount of energy is deposited into the thermalized molecules. Initial electronic excitation is rapidly converted to vibrational excitation, and the vibrationally excited molecules dissociate. The ground state of $Co(H_2O)_4^{2+}$ was calculated to lie 21 kJ/mol above the ground state of the charge separated products.[14] $Co(H_2O)_4^{2+}$ is, however, kinetically stable because of the large Coulomb barrier that separates it from the products.

In the present work, we have located the salt-bridge transition state geometry with high-level DFT methods and calculated the height of the reverse activation barrier of the title reaction:

$$Co(H_2O)_4^{2+} \rightarrow CoOH(H_2O)_2^{+} + H_3O^{+} \qquad (3)$$

Differences between the calculated barrier height and the measured KER are discussed, as well as the onset of Coulomb explosion at the transition state geometry using the imaginary vibrational mode.

Computational Details

The calculations were performed with the Gaussian 98 program package,[16] employing the B3LYP[17] density functional method together with the 6-311++G(3df,3pd) basis set on oxygen and hydrogen and the SDD[18] relativistic effective core potential basis set on cobalt, as incorporated in the program. To locate the transition state, an H_3O^{+} unit was attached to a preoptimized $CoOH(H_2O)_2^{+}$ fragment, taking the respective geometry parameters from earlier calculations of the corresponding $MgOH^{+}-H_3O^{+}$ transition state.[11] The geometry was

* To whom correspondence should be addressed. E-mail: martin.beyer@ch.tum.de. E-mail: rbmetz@chemistry.umass.edu.

10.1021/jp027031w CCC: $25.00
Published on Web 02/20/2003

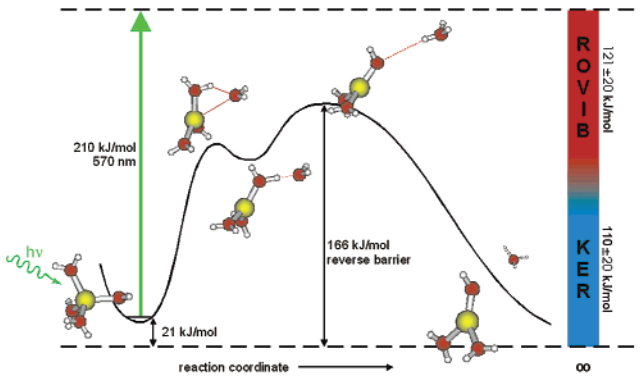

Figure 1. Reaction path for the dissociation of $Co(H_2O)_4^{2+}$ to $CoOH(H_2O)_2^{+} + H_3O^{+}$ along with the partitioning of the available energy. Excitation with 570 nm laser light deposits 210 kJ/mol in the $Co(H_2O)_4^{2+}$ complex as electronic excitation. Rapid internal conversion results in a highly vibrationally excited molecular ion.[14] In the first step toward charge separation, one water ligand moves to the second solvation shell, going through a transition state to a local minimum on the potential energy surface. Subsequently, a proton is transferred between the first and second solvation shell water molecules, followed by Coulombic explosion of the complex. Only 110 ± 20 kJ/mol is released as kinetic energy (KER);[14] the remaining 121 ± 20 kJ/mol goes into rotational and vibrational excitation (ROVIB) of the products. Possible mechanisms for the conversion of potential into vibrational and rotational energy are discussed in the text.

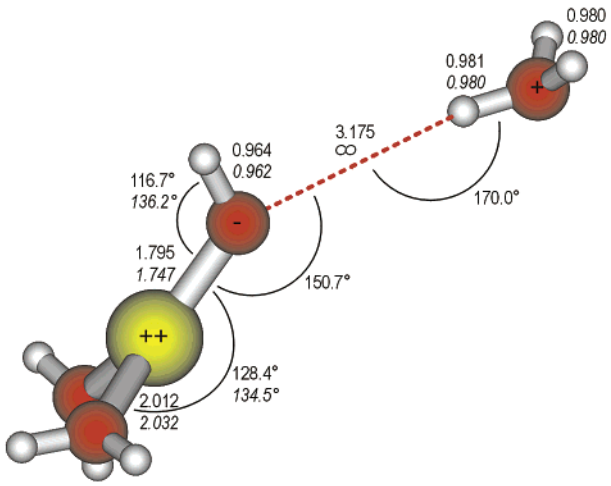

Figure 2. Transition state geometry of $Co(H_2O)_4^{2+}$ before Coulombic explosion to $CoOH(H_2O)_2^{+} + H_3O^{+}$. Color coding is yellow for Co, red for O, and gray for H. Distances are in angstrom. The italic number is the corresponding parameter in the fully separated and relaxed products. Major changes from the transition state to the products are the increased Co−O−H angle and the reduced Co−O bond in the $CoOH^{+}$ moiety, whereas the H_3O^{+} geometry does not change significantly. The H_3O^{+} unit is already well separated from the hydrated hydroxide $CoOH(H_2O)_2^{+}$ by more than 3 Å, so it is conceivable that the interaction is purely Coulombic. The major charge centers, Co^{2+}, OH^{-}, and H_3O^{+}, are in almost linear arrangement in the transition state. This salt-bridge structure minimizes the Coulomb barrier of the reaction.

preoptimized with a smaller basis on O and H atoms before it was brought to full convergence at the target level of theory. The stability of the electronic wave function was confirmed with the *stable* option of Gaussian 98. A frequency calculation confirmed the transition state. Errors in the calculated energies are expected to be on the order of 10 kJ/mol.[19]

Results and Discussion

Figure 1 illustrates the complete reaction path together with the partitioning of the available energy. Upon excitation with 570 nm laser light, 210 kJ/mol is deposited in the complex as electronic excitation, presumably followed by rapid internal conversion, leaving the molecular ion in a vibrationally highly excited state. As the first step toward charge separation, one water ligand moves to the second solvation shell, reaching a local minimum on the potential energy surface. Subsequently, a proton is transferred between the first and second solvation shell water molecules, followed by Coulombic explosion of the complex. Our calculations for these three stationary points on the potential energy surface indicate that the first barrier lies below the second; that is, the salt-bridge transition state determines the activation energy.

The geometry of this salt-bridge transition state is depicted in Figure 2. Key geometry parameters are given in angstroms and degrees, the respective values in the fully separated fragments are given in italics for comparison. The complete geometry is available in the Supporting Information. The H_3O^{+} geometry is basically unaffected by the presence of $CoOH(H_2O)_2^{+}$, whereas the latter undergoes some deformations to adapt to the transition state geometry. The most pronounced effect is the tilting of the OH^{-} moiety by ∼20° at the TS, as its H atom feels repulsive interactions both from the Co^{2+} and the H_3O^{+} charge centers. With a 150.7° angle between the $Co^{2+}-OH^{-}$ bond and the $H_3O^{+}-OH^{-}$ long-range interaction, an almost linear $Co^{2+}-OH^{-}-H_3O^{+}$ salt-bridge is present at the transition state. The difference in Coulomb energy between the transition state geometry and the product, with a charge distribution as indicated in Figure 2, is a physical estimate of the reverse activation energy, as outlined previously.[11] Using eq 8 from ref 11, one obtains a value of 192 kJ/mol, which lies 26 kJ/mol above the quantum chemical result. This is a reasonable value, because the simple picture of interacting double and single charges neglects the shielding effect of the two additional solvent molecules.

Figure S1, an animated GIF, shows the motion of the imaginary vibrational mode of 69*i* cm^{-1}, which corresponds to the movement of the molecule along the reaction coordinate. The salt-bridge transition state separates the attractive from the repulsive part of the $CoOH(H_2O)^{+}-H_3O^{+}$ interaction potential. $Co(H_2O)_4^{2+}$ with one water in the second solvation shell, $Co(H_2O)_3(H_2O)^{2+}$, transfers a proton from the inner-shell to the outer-shell water, as the outer-shell water departs. Separation of the fragments beyond the transition state geometry results in a Coulombic explosion. Figure S1 shows that, during the dissociation, the H_3O^{+} unit picks up considerable angular momentum, converting potential into rotational energy. This rotation is already indicated in the transition state geometry, in which the OH bond in H_3O^{+} is tilted against the long-range bond. This tilt is probably caused by the attractive interaction of the Co^{2+} with the negative end of the H_3O^{+} dipole. At the onset of the Coulombic explosion, the overall repulsion between the fragments and the attraction between the Co^{2+} charge center and the H_3O^{+} dipole overlap. The dominant interaction is the charge−charge repulsion, whereas the weaker charge-dipole attraction causes the observed torque.

How reasonable is it that, of a total available energy of 231 kJ/mol, only 110 kJ/mol[14] goes into kinetic energy release, whereas 121 kJ/mol ends up in vibrational and rotational excitation of the products? It is quite obvious that significant excess energy has to be present in order to achieve the experimentally observed dissociation rate of more than 2×10^{7} s^{-1}. Yet one might very well argue that, if the reverse activation barrier is 166 kJ/mol, the measured KER should be at least 166 kJ/mol, because some of the 65 kJ/mol excess energy should

result in kinetic energy of the products, in addition to the energy gained in the Coulombic explosion. However, the ground-state $Co(H_2O)_4^{2+}$ has 33 vibrational degrees of freedom, of which all but the water stretching and bending modes are low frequency and excellent energy sinks. To push the complex over the barrier, at least 145 kJ/mol out of the 210 kJ/mol photon energy, i.e., 70%, has to be partitioned into the reaction coordinate. Because about 20 low frequency modes are available to absorb the remaining 30%, we consider it highly unlikely that significant energy in excess of the barrier will be present in the reaction coordinate. We therefore assume that the reverse barrier of zero-point-corrected $\Delta D_0 = 166 \pm 10$ kJ/mol provides an upper limit to the kinetic energy release in the Coulombic explosion.

To bring the calculations in agreement with the experiment, a difference of 56 ± 30 kJ/mol between the calculated barrier and the measured KER has to be rationalized. One possible energy sink is the relaxation of the fragments to their equilibrium geometry, which converts potential into vibrational energy. To quantify this effect, we calculated the energy of the $CoOH(H_2O)_2^+$ and the H_3O^+ units in the geometry they adopt at the transition state. The geometry change in the H_3O^+ unit is small, and consequently, the energy change is only 0.05 kJ/mol and therefore negligible. The situation is quite different for the $CoOH(H_2O)_2^+$ fragment, which lies 5.7 kJ/mol higher in energy when deformed to the transition state geometry. During the Coulombic explosion, the $CoOH(H_2O)_2^+$ relaxes, and this 5.7 kJ/mol is most likely released as vibrational excitation into the molecule.

Some of the available energy goes to rotation, especially of the H_3O^+ product, which is a result of the multipole interaction of the two units in the transition state, as discussed above. Probably the largest factor in reducing the observed kinetic energy release, however, is the fact that the calculations are done on equilibrium geometries, whereas in the experiment, the complex is highly vibrationally excited. In the transition state, an excess energy of 65 kJ/mol is heating the complex, which is sufficient to populate most of the vibrational modes. Because especially the low frequency modes are anharmonic, the geometry of the transition state that the molecule actually passes through will differ significantly from the calculated stationary point on the potential energy surface. The predominant effect will be an increase of the bond distances, and because the interaction is largely Coulombic, its magnitude will be reduced.

Applying the same argument in a more dynamical picture, one may consider the effect of the two spectator water ligands on the dissociation. If the H_3O^+ escapes in a moment when one of the vibrating spectator ligands is shielding the Co^{2+} more effectively than in the calculated transition state, the repulsive interaction would be less pronounced, and the reverse barrier might be lowered significantly.

Unfortunately, we are not able to quantify most of the effects which contribute to the difference between the measured KER and the calculated reverse barrier. On the basis of the arguments presented, we consider it likely that each of the effects—product relaxation, rotation, geometry change, and shielding—contributes 5−15 kJ/mol. Not one of the effects alone but all of them together are capable of explaining the 56 ± 30 kJ/mol difference between experiment and theory.

Conclusion

The calculated transition state geometry and energetics confirm the earlier interpretation of photodissociation experiments of $Co(H_2O)_4^{2+}$ in terms of a salt-bridge mechanism. We have linked quantitative kinetic energy release measurements to the calculated reverse activation barrier of the dissociation. Charge reduction in doubly charged metal ions solvated with multiple molecules of a protic solvent proceeds via a transition state in which the charge centers are in a salt-bridge arrangement. This lowers the activation energy of the dissociative proton transfer between a first and second shell solvent molecule. Dissociative proton transfer is in fact the only type of charge reduction reaction which is observed in these systems.

Acknowledgment. Generous financial support by the Leonhard-Lorenz-Foundation (M.K.B.) and by the donors of the Petroleum Research Fund administered by the American Chemical Society (R.B.M.) is gratefully acknowledged.

Supporting Information Available: Figure S1 (animated GIF). Coordinates and Gaussian 98[16] thermochemistry output of optimized structures (RTF). This material is available free of charge via the Internet at http://pubs.acs.org.

References and Notes

(1) Fenn, J. B.; Mann, M.; Meng, C. K.; Wong, S. F.; Whitehouse, C. M. *Science* **1989**, *246*, 64.

(2) Jayaweera, P.; Blades, A. T.; Ikonomou, M. G.; Kebarle, P. *J. Am. Chem. Soc.* **1990**, *112*, 2452.

(3) Blades, A. T.; Jayaweera, P.; Ikonomou, M. G.; Kebarle, P. *J. Chem. Phys.* **1990**, *92*, 5900.

(4) Blades, A. T.; Jayaweera, P.; Ikonomou, M. G.; Kebarle, P. *Int. J. Mass Spectrom. Ion Processes* **1990**, *102*, 251.

(5) Schmelzeisen-Redeker, G.; Bütfering, L.; Röllgen, F. W. *Int. J. Mass Spectrom. Ion Processes* **1989**, *90*, 139.

(6) Stace, A. J. *J. Phys. Chem. A* **2002**, *106*, 7993.

(7) Shvartsburg, A. A.; Siu, K. W. M. *J. Am. Chem. Soc.* **2001**, *123*, 10071.

(8) Spears, K. G.; Fehsenfeld, F. C.; McFarland, M.; Ferguson, E. E. *J. Chem. Phys.* **1972**, *56*, 2562.

(9) Solà, M.; Lledós, A.; Duran, M.; Bertrán, J. *Theor. Chim. Acta* **1992**, *81*, 303.

(10) Peschke, M.; Blades, A. T.; Kebarle, P. *Int. J. Mass Spectrom.* **1999**, *185*, 685.

(11) Beyer, M.; Williams, E. R.; Bondybey, V. E. *J. Am. Chem. Soc.* **1999**, *121*, 1565.

(12) Vitorge, P.; Masella, M. *Chem. Phys. Lett.* **2000**, *332*, 367.

(13) Bondybey, V. E.; Beyer, M. K. *Int. Rev. Phys. Chem.* **2002**, *21*, 277.

(14) Faherty, K. P.; Thompson, C. J.; Aguirre, F.; Michne, J.; Metz, R. B. *J. Phys. Chem. A* **2001**, *105*, 10054.

(15) Thompson, C. J.; Husband, J.; Aguirre, F.; Metz, R. B. *J. Phys. Chem. A* **2000**, *104*, 8155.

(16) Frisch, M. J.; Trucks, G. W.; Schlegel, H. B.; Scuseria, G. E.; Robb, M. A.; Cheeseman, J. R.; Zakrzewski, V. G.; Montgomery, J. A., Jr.; Stratmann, R. E.; Burant, J. C.; Dapprich, S.; Millam, J. M.; Daniels, A. D.; Kudin, K. N.; Strain, M. C.; Farkas, O.; Tomasi, J.; Barone, V.; Cossi, M.; Cammi, R.; Mennucci, B.; Pomelli, C.; Adamo, C.; Clifford, S.; Ochterski, J.; Petersson, G. A.; Ayala, P. Y.; Cui, Q.; Morokuma, K.; Malick, D. K.; Rabuck, A. D.; Raghavachari, K.; Foresman, J. B.; Cioslowski, J.; Ortiz, J. V.; Stefanov, B. B.; Liu, G.; Liashenko, A.; Piskorz, P.; Komaromi, I.; Gomperts, R.; Martin, R. L.; Fox, D. J.; Keith, T.; Al-Laham, M. A.; Peng, C. Y.; Nanayakkara, A.; Gonzalez, C.; Challacombe, M.; Gill, P. M. W.; Johnson, B. G.; Chen, W.; Wong, M. W.; Andres, J. L.; Head-Gordon, M.; Replogle, E. S.; Pople, J. A. *Gaussian 98*, revision A.7; Gaussian, Inc.: Pittsburgh, PA, 1998.

(17) Becke, A. D. *J. Chem. Phys.* **1993**, *98*, 5648.

(18) Dolg, M.; Wedig, U.; Stoll, H.; Preuss, H. *J. Chem. Phys.* **1987**, *86*, 866.

(19) Glukhovtsev, M. N.; Bach, R. D.; Nagel, C. J. *J. Phys. Chem. A* **1997**, *101*, 316.